ADVANCED OPERATIONAL MODELS OF THE APPLE X UNDULATOR

X. Liang[*,1,2], M. Calvi[1], C. Kittel[1,3], T. Schmidt[1] and N. J. Sammut[3]
[1]Paul Scherrer Institut, 5232 Villigen PSI, Switzerland
[2]Paris-Sud University, 91400 Orsay, France
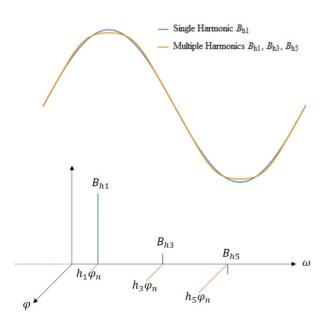[3]University of Malta, Msida, Malta

Abstract

Athos is a new soft X-ray beamline at SwissFEL, where the Apple X type undulators will be equipped. These devices are flexible to produce light in different polarization modes. An adequate magnetic field model is required for the operation of undulator. The undulator deflection parameter K and its gradient are calculated starting from the Fourier series of the magnetic field. In the classical parallel and anti-parallel operational modes - respectively elliptical and linear modes, the variation of the magnetic field as well as its parameters are evaluated by computer modeling. The results are compared to the magnetic measurements of the first Apple X prototype.

INTRODUCTION

16 Apple X undulators will be installed on Athos Beamline. Each one contains 800 magnets distributed in a Halbach configuration in 4 arrays (see Fig. 1 top right). Motors are equipped to move the arrays longitudinally and radially. The different operational modes of the undulator are defined by the way of longitudinal shifting of the arrays.

___

* xiaoyang.liang@psi.ch, xiaoyang.liang@u-psud.fr

In parallel mode, the opposite arrays are shifted in same direction. The polarization of light changes its elliptical form. While in anti-parallel mode, we move the opposite arrays in different direction, which turns the polarization axes of the photon beam. Moreover, by changing the radial gap between the arrays, we are able to adjust the magnetic strength.

During the parallel mode, the K value variation (see Fig. 2) in the measurement results is not able to be explained with the previous magnetic (single harmonic) model. An updated and adapted physical model with higher harmonics of the Fourier series was proposed. The correction was applied for the non-sinusoidal magnetic field. The analysis of the influence of the high harmonic coefficients are mainly discussed in this contribution. The calculation result indicates that the updated model is not enough to describe the phenomenon. Further discussion about the K value variation will be carried out in the last part.

UPDATED MAGNETIC FIELD MODEL

The convention of the coordinate system of the magnetic field composes a transverse plane (x,y) along with its longitudinal position z. The horizontal and vertical components of the magnetic field are named as B_x and B_y respec-
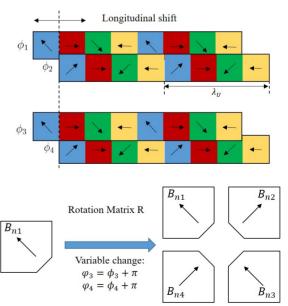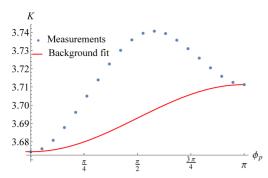

Figure 1: Top left: Example of a non-sinusoidal field correction with multiple harmonics. Top right: Scheme of the longitudinal shift of 4 arrays (Circular mode as an example). Bottom left: Scheme of simplified expression of the magnetic field in Fourier domain. Bottom right: Using the mathematical tools to express 4 arrays as a function of the first array.

Figure 2: Measurement result of K value variation in parallel mode.

tively. On the reference electron beam orbit, equally speaking $(x, y) = (0,0)$, the non-sinusoidal and periodical magnetic field of a single array can be expressed with a series. We take the example of B_x component:

$$B_x(z) = \sum_{h=1,3,5} B_{xh} \cos\left(h\frac{2\pi}{\lambda_u}z + \phi_n\right) \qquad (1)$$

The different harmonic orders of the series are noted as h. Using only the first 3 odd harmonic orders is enough for the theoretical analysis. λ_U is the undulator period. ϕ_n is the relative longitudinal phase shift of the nth array. (see Fig. 1 top right).

With the simplified expression in the Fourier domain and the rotation matrix [1] (see Fig. 1 bottom left and bottom right), we are able to express the whole field of 4 arrays as a function of harmonic coefficients of one array and longitudinal phase shifts:

$$\hat{\boldsymbol{B}}\left(\hat{\boldsymbol{B}}_{1h}, \phi_1, ...\right) = \sum_{h=1,3,5} \sum_{n=1}^{4} \exp(ih\phi_n)\boldsymbol{R_n} \cdot \hat{\boldsymbol{B}}_{1h} \qquad (2)$$

where $\hat{\boldsymbol{B}}_{1h}$ is a vector in transverse plan. (^) means that the parameters could be complex due to the expression in the Fourier domain, $\boldsymbol{R_n}$ is the rotation matrix. The advantage of this complex expression is to simplify the calculation of the K value and its gradient. Comparing the previous and the updated model with the measurement results (see Fig. 3 and Fig. 4) show that the updated magnetic model is more reliable.

K VALUE AND ITS GRADIENT

The undulator associated deflection parameter K of a non-sinusoidal magnetic field [2] is expressed:

$$K_{eff} = \kappa \sqrt{\sum_{h=1,3,5}\left(b_{xh}^2 + b_{yh}^2\right)} \qquad (3)$$

where we define: $\kappa = \frac{e\lambda_u}{2\pi m_e c}$ and $b_h = \frac{B_h}{h}$.
Eq.(3) in complex form is updated as:

$$K_{eff}^2 = \sum_{h=1,3,5} \hat{\boldsymbol{K}}_h \cdot \hat{\boldsymbol{K}}_h^* \qquad (4)$$
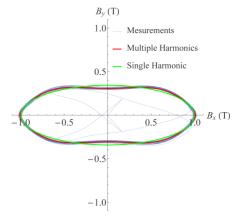
Figure 3: During the parallel mode: Transverse magnetic field distribution along z in elliptical polarization case.
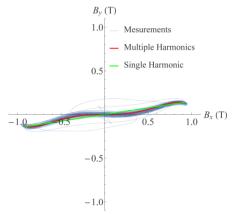

Figure 4: During the anti-parallel mode: Transvers magnetic field distribution along z in the case of linear polarization with certain angle.

where $\hat{\boldsymbol{K}}_h$ is also a vector in transverse plan: $(\hat{K}_{xh}, \hat{K}_{yh}) = \kappa\frac{\hat{\boldsymbol{B}}_h}{h} = \kappa\hat{\boldsymbol{b}}_h$.

For the simplification of the calculation, we define a $\boldsymbol{Z_h}$ matrix as a combination of the rotation matrix R_n and longitudinal phase shifts:

$$\varphi_1 = \phi_1, \quad \varphi_2 = \phi_2, \quad \varphi_3 = \phi_3 + \pi, \quad \varphi_4 = \phi_4 + \pi$$

$$Z_{xh} = e^{ih\varphi_1} - e^{ih\varphi_2} + e^{ih\varphi_3} - e^{ih\varphi_4}$$
$$Z_{yh} = e^{ih\varphi_1} + e^{ih\varphi_2} + e^{ih\varphi_3} + e^{ih\varphi_4}$$
$$\boldsymbol{Z_h} = \begin{bmatrix} Z_{xh} & 0 \\ 0 & Z_{yh} \end{bmatrix}$$

The 4 arrays are in the linear horizontal polarization mode (pure vertical field) when $\varphi_1 = \varphi_2 = \varphi_3 = \varphi_4 = 0$. After the change of variables between ϕ and φ, the magnetic field distribution in the model matches closer the magnetic field of the real undulator.

Then the formula (4) can be expressed as:

$$K_{eff} = \kappa \sqrt{\sum_{h=1,3,5} [(\boldsymbol{Z_h} \cdot \hat{\boldsymbol{b}}_{1h})^T \cdot (\boldsymbol{Z_h} \cdot \hat{\boldsymbol{b}}_{1h})^*]} \qquad (5)$$

In parallel mode, we shift relatively arrays No.1 and No.3 in the same direction - the polarization of the photon beam changes its elliptical form. The relative shift phase differences of the arrays vary thus in this way:

$$\varphi_1 = \phi_p, \quad \varphi_2 = 0, \quad \varphi_3 = \phi_p, \quad \varphi_4 = 0$$

With the Z_h matrix, the number of the array doesn't play a role anymore, we can note b_{1h} as b_h. We obtain then K_{eff} in parallel operational mode:

$$K_{eff}(\phi_P) = 2\sqrt{2}\kappa \sqrt{\sum_{h=1,3,5}(b_{xh}^2 + b_{yh}^2) - \cos(h\phi_P)(b_{xh}^2 - b_{yh}^2)} \tag{6}$$

Implementing the empirical value of b_x and b_y for each harmonic into the Eq. (6), we are able to compare the difference before and after the update with higher harmonics (see Fig. 5). The relative correction is on a level of 10^{-5}.
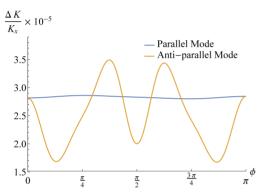

Figure 5: Correction of K value variation with multiple harmonics compared to the single harmonic case.

The anti-parallel mode is able to change the polarization axes of the photon beam. We shift the opposite array No.1 and No.3, or No.2 and No.4, in different direction. The phase shifts vary accordingly:

$$\varphi_1 = \phi_{\bar{p}}, \quad \varphi_2 = 0, \quad \varphi_3 = -\phi_{\bar{p}}, \quad \varphi_4 = 0$$

The equation of the K variation as a function of $\phi_{\bar{p}}$ in anti-parallel mode is more complicated. Therefore, we only show the simulation result in Fig. 5 together with the result of the parallel mode. The variation in anti-parallel mode is much more important. However, the correction is still on a level of 10^{-5}. The coefficients b_3 and b_5 have not enough influence to create a difference on a level of 1%, which is the case of the measurement (see Fig. 2).

The updated equation of the transverse gradient of K is:

$$\nabla K = \frac{\kappa^2}{K_{eff}} \sum_{h=1,3,5} \Re(\hat{J}_h \cdot \hat{b}_h^*) \tag{7}$$

where $\hat{J}_h$ is the Jacobian: $\hat{J}_h = \begin{bmatrix} \partial_x \hat{B}_{xh} & \partial_y \hat{B}_{xh} \\ \partial_x \hat{B}_{yh} & \partial_y \hat{B}_{yh} \end{bmatrix}$.

MEASUREMENT AND ANALYSIS

The measurement result in Fig. 2 is reproducible on a level of about 10^{-5}. To operate the undulator for the beamline [3], we need to fit the measurement points to satisfy the precision requirement of 10^{-4}. Based on the analysis of the multiple harmonics update for the physical model, the single harmonic model is enough. The background part can be fitted by the old model. The residual part, called corrective part for fitting, can be well fitted with a model in form of $\sin^2(\phi)$.

This residual part of the K value variation has not yet been fully understood. However, the analysis in Fig. 6 shows that it is strongly related to the magnetic strength. It decreases faster than the magnetic field versus the radial gap between the arrays.
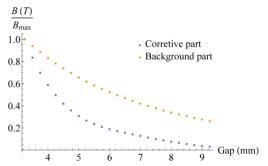

Figure 6: The relative amplitude of the fitted b_1 and the coefficient of the corrective function $\sin^2(\phi)$ versus gap of 4 arrays.

CONCLUSION

The higher harmonics of the magnetic field of the Apple X undulator make a difference on a level of 10^{-5} for the K value variation during different operational modes. These modeling results suggest that the variation of K at a level of 1% is not related to the higher harmonics. We have not fully understood this behavior yet. A further analysis indicates that the mechanical deformation could be the reason of this unknown effect. However, with empirical characterizations and fits, we can handle this problem for operation. The measurements about the mechanical deformation is being carried out in order to find an explanation.

ACKNOWLEDGEMENTS

REFERENCES

[1] M. Calvi *et al.*, "Transverse gradient in Apple-type undulators", *J. Synchrotron Rad.*, vol. 24, pp. 600-608, 2017. doi:10.1107/S1600577517004726

[2] M. Calvi *et al.*, *Magnetic assessment and modelling of the Aramis undulator beamline*, *J. Synchrotron Rad.*, vol. 25, pp. 686-705, 2018. doi:10.1107/S1600577518002205

[3] C. Kittel, M. Calvi, X. Liang, T. Schmidt, and N. J. Sammut, "Operational Model of the Athos Undulator Beamline", presented at the FEL'19, Hamburg, Germany, Aug. 2019, paper WEP097.

WEP098

Photon Beamline Instrumentation and Undulators